IEEE Access
Multidisciplinary | Rapid Review | Open Access Journal

Received 26 April 2024, accepted 13 May 2024, date of publication 17 May 2024, date of current version 24 May 2024.

Digital Object Identifier 10.1109/ACCESS.2024.3402240

APPLIED RESEARCH

One-Dimensional Elastic and Viscoelastic Full-Waveform Inversion in Heterogeneous Media Using Physics-Informed Neural Networks

ALIREZA PAKRAVAN
Department of Mechanical Engineering, San Diego State University, San Diego, CA 92182, USA
e-mail: apakravan@sdsu.edu

ABSTRACT In this study, we discuss a mathematical framework to handle the inverse problem for the applications of partial differential equations (PDEs). In particular, we focus on wave equations and attempt to identify the wave parameters such as wave velocity from scant measurements of the domain's response to prescribed initial conditions. To this end, we need an algorithm to play the role of inverse PDE solver for full-waveform inversion. Over the past several years, multilayer neural networks have been developed and applied to a broad range of problems in applied mathematics and physics. Specifically, Physics Informed Neural Network (PINN) as a novel technique has been proposed recently for solving partial differential equations. In PINN's algorithm, the mesh generation effort is not necessary as it is for any other numerical discretization method. The algorithm just needs a batch of points in which to apply the conditions set in the loss function. We employ PINN for solving the wave equations during the inversion process. The first objective of this research is to develop a robust and efficient algorithm based on PINN for the reconstruction of the wave velocity profile in heterogeneous media. Continuous and piecewise continuous functions are considered for the wave velocity target profiles. Next, we are interested in performing the inversion process of the wave equation in semi-infinite heterogeneous media which is one of the major advantages of the PINN in contrast to traditional numerical approaches. The last objective is to simultaneously recover the parameters of the viscously damped wave equation in heterogeneous domains. The effect of noisy measured response on the inversion process is also investigated.

INDEX TERMS Heterogeneous media, inverse problem, noisy measured response, partial differential equation, physics informed neural network, wave equations.

I. INTRODUCTION

In recent decades, advances in mathematical algorithms [1], [2], [3], [4], data acquisition systems, and computer hardware have renewed hope for identifying the physical (material) parameters of a mathematical model with minimum given information. From a mathematical point of view, at the center of such problems lies, typically, an inverse problem. That is, a problem, for example, where the geometry of the domain, the boundary and initial conditions of the domain, and the domain's response i.e. displacement at some stations may be known, but the domain's material composition is unknown. There are plenty of developments aiming at the solution of such a mathematically and computationally challenging inverse problem that recently arises in various applications [5], [6], [7], [8].

The associate editor coordinating the review of this manuscript and approving it for publication was Hengyong Yu.

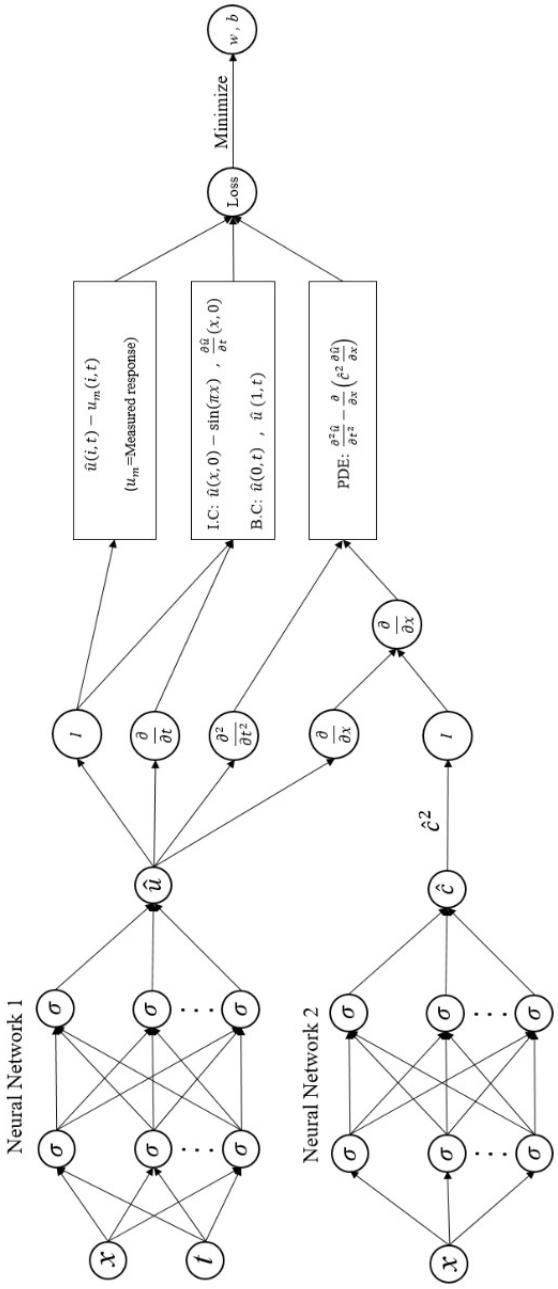

FIGURE 1. Schematics of PINNs' workflow for solving full waveform inversion in heterogeneous media.

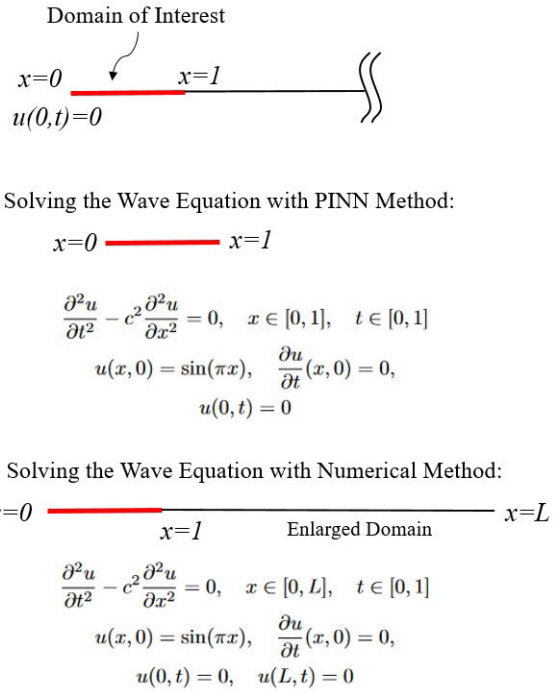

FIGURE 2. Comparison between PINN and numerical methods to solve wave equation in a domain of interest embedded in semi-infinite media.

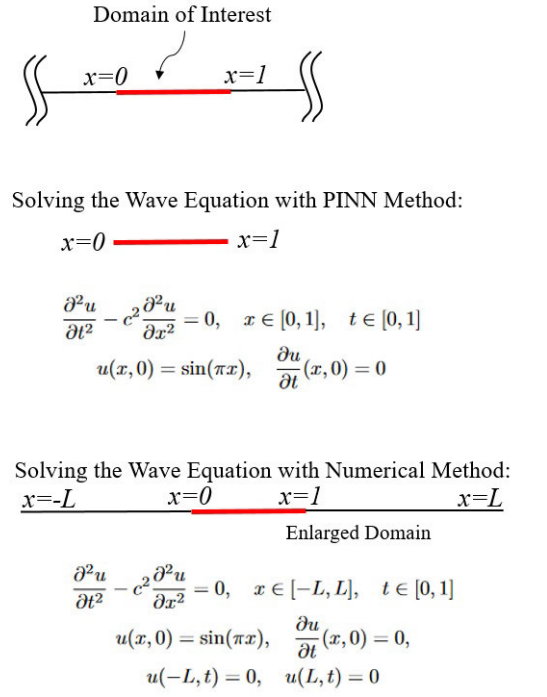

FIGURE 3. Comparison between PINN and numerical methods to solve wave equation in a domain of interest embedded in infinite media.

Inverse problems involving the simulation of waves to reconstruct elastic and viscoelastic material in heterogeneous finite, semi-infinite, and infinite domains find applications in many science and engineering disciplines. In this study, we focus on one dimensional wave equation and attempt with the reconstruction of the spatially-distributed material properties of a domain such as wave velocity and wave-attenuation by leveraging the medium's response to interrogating waves. Mathematically, the problem entails the identification of the spatially dependent coefficients of the partial differential equation (PDE) governing the physics of the problem (wave equation). The PDE coefficients may be either scalars, continuous or piecewise continuous functions.

In general, the inverse problems have solutions that may not be unique and may not depend continuously on the given

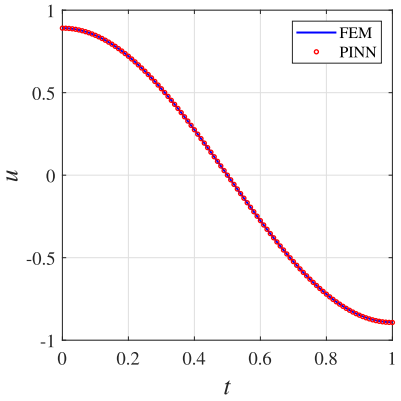

FIGURE 4. u **Sampled at** $x = 0.35$.

effects [9], [10], [11], [12], [13], [14]. Hence the inverse problems are typically ill-posed and are difficult to solve. To find the optimal solution of the inverse problem and handle the ill-posedness, appropriate iterative techniques need to be applied [12], [15], [16], [17], [18], [19], [20], [21], [22], [23], [24]. Even in inverse-PDE problems, we must solve the PDE as a direct problem in each iteration. In some rare cases, yet useful, there exists an analytic-exact solution to the PDEs. Nevertheless, some type of numerical methods are required to be employed for the vast majority of solving PDE for many applied math applications. Finite element method (FEM) [25] and finite difference method (FDM) [26] are two common examples of the numerical approximation techniques.

The domain discretization is the idea behind these numerical approaches. The computational domain of interest where our PDE are to be solved is divided to some sub-regions, and based on the numerical approximation, we find the solution on each of these sub-regions. Putting together these individual solutions will be resulted in the final solution of the computational domain. The procedure to find the solution of PDE targets to minimize the approximation error, and the solution provides different properties depending on what numerical method we utilize. Also, the accuracy of the solution depends on the chosen discretization mesh for the domain. A fine mesh as a level of precision of the discretization causes the computational costs for some applications with large scale of interest domain [27], [28].

Advances in computing power and rapid growth of available data in recent years have invigorated the field of neural networks and data science [29], [30], [31], [32], [33]. The most notable architecture within neural networks is multilayer neural networks [34], [35], [36], [37], [38], [39], [40], [41], [42] which have achieved exceptional results in a wide range of problems. Although the theory to train neural networks has been available since the early 60's [35], [43], [44], it has recently become possible to train them on commonly available hardware. Typical applications of neural networks employ these networks to recover functions that are not directly available to the user. For example in image recognition, functions that map images to the corresponding classes are vastly complex and high dimensional functions.

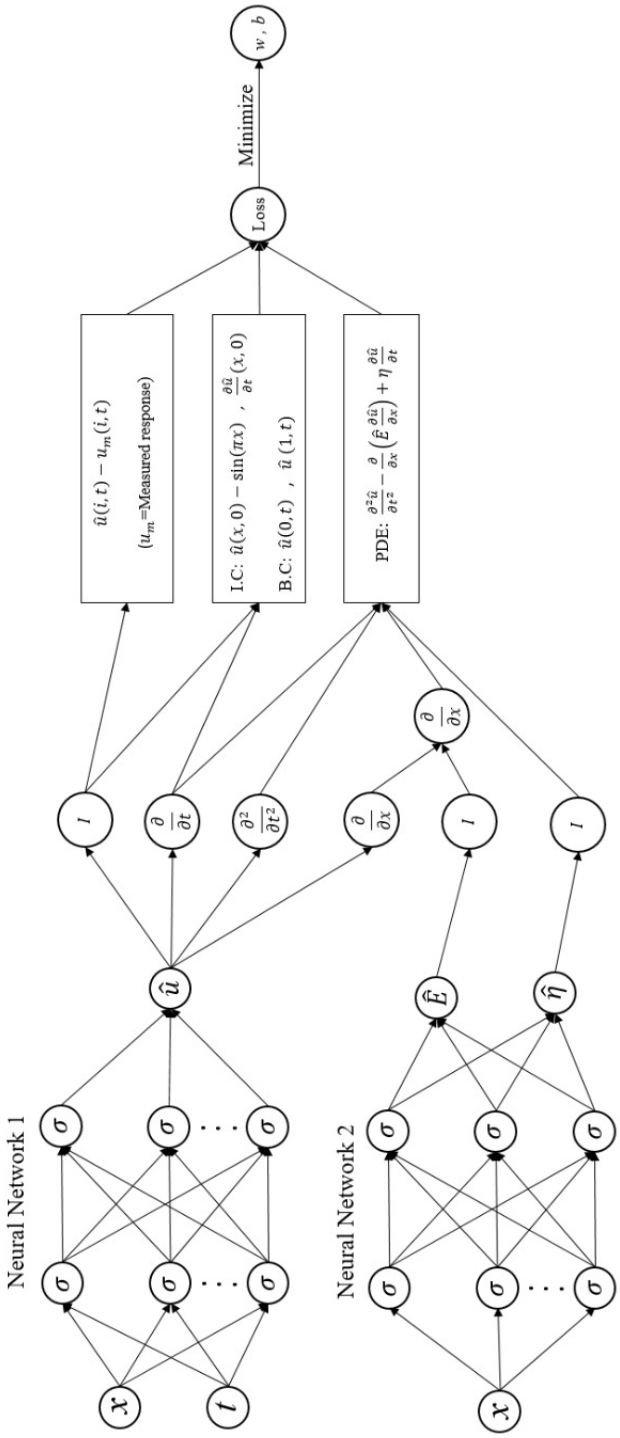

FIGURE 5. **Schematics of PINNs' workflow for solving full waveform inversion of viscously damped motion in heterogeneous media.**

PDE is another problem that many researchers have been interested in finding unknown functions by neural networks. As we mentioned, numerical methods divide the geometry of the PDE into simple elements and compute an approximated

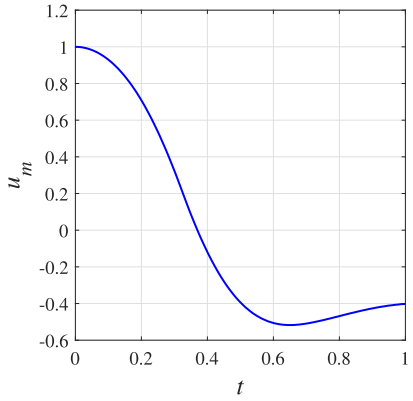

FIGURE 6. Measured displacement response $u_m(0.5, t)$.

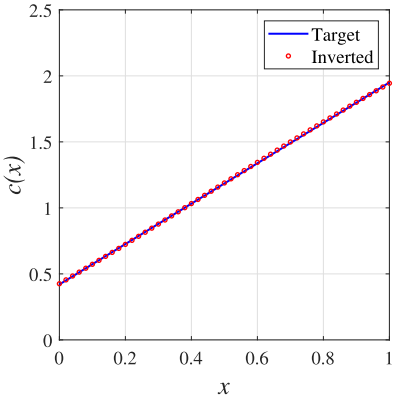

FIGURE 7. Target and inverted wave velocity profiles.

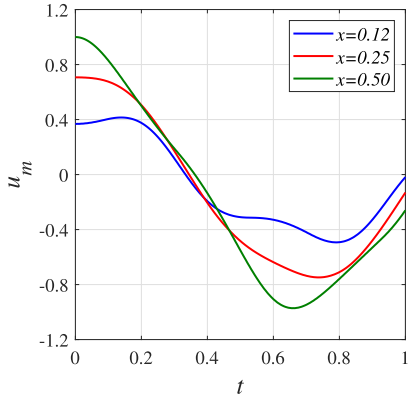

FIGURE 8. Measured displacement responses at three stations.

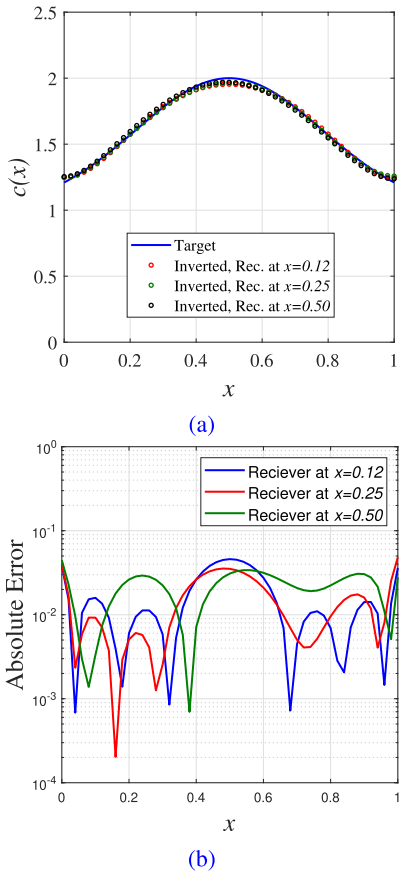

FIGURE 9. (a): Target and inverted wave velocity profiles, (b): Absolute error.

solution on these elements using basis or shape functions. The neurons in a neural networks can also be assumed as kind of basis functions. The first study [45] in this context shows that neural networks are closed form expressions, and thus provide information about the approximation anywhere in the relevant domain. This information includes derivatives of the solution, as neural networks with the appropriate activation functions are differentiable functions. Furthermore, they state that training neural networks is a highly parallelizable process.

Physics informed neural networks (PINN) [46] as a novel technique is recently presented for solving the differential equations. This approach stems from multilayer neural network's capacity to be universal function approximators [34] and continuous improvements in automatic differentiation [47] to calculate gradients of the neural network's outputs with respect to its inputs. These features easily help us to model the PDEs. This method solves the obtained PDE directly through the loss function. In fact, the formulation is such that neural networks are parametric trial solutions of the differential equation, and the loss function accounts for errors with respect to initial/boundary conditions and collocation points. After introducing PINNs, a large variety of studies in many applications have been prompted so far such as Cai et al. [48] in heat transfer, Jin et al. [49] and Rodriguez-Torrado et al. [50] in fluid mechanics, Mao et al. [51] in high speed flows, Jagtap et al. [52] in supersonic flows, Haghighat et al. [53] in solid mechanics, and Xu et al. [54] in geophysic. For review of other applications/problems of PINNs, see [55], [56], [57], [58], [59], [60], [61], [62]

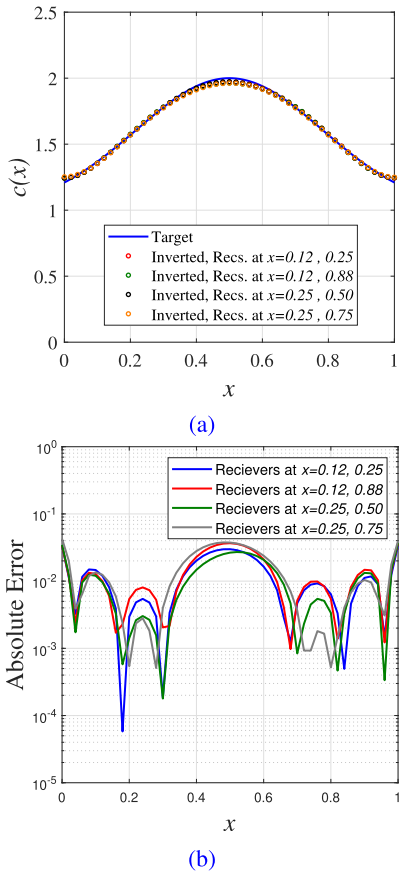

FIGURE 10. (a): Target and inverted wave velocity profiles, (b): Absolute error.

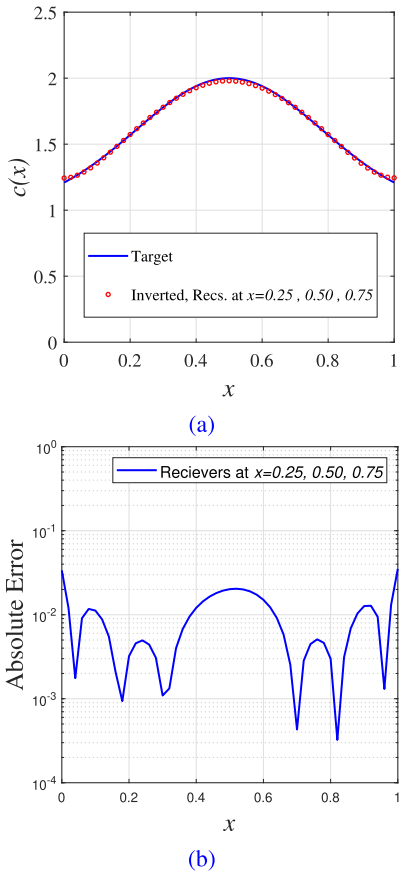

FIGURE 11. (a): Target and inverted wave velocity profiles, (b): Absolute error.

TABLE 1. L^2 norm error in the recovered c for different locations of receivers.

Location (x)	L^2 norm
0.12	0.1527
0.25	0.1371
0.50	0.1683
0.12 , 0.25	0.1099
0.12 , 0.88	0.1275
0.25 , 0.50	0.1048
0.25 , 0.75	0.1385
0.25 , 0.50 , 0.75	0.0882

TABLE 2. L^2 norm error in the recovered c for different locations of receivers.

Location (x)	L^2 norm
0.12	0.0422
0.25	0.0238
0.50	0.0675
0.12 , 0.88	0.0188
0.25 , 0.50	0.0228
0.25 , 0.75	0.0138

The advantage of PINN is not limited to direct solving the partial differential equations. This algorithm is also valid to solve inverse problems. In other words, using PINN, we concern to identify unknown parameters of PDE in presence of some measured responses. The inverse problem is what this study focuses on. It consists of discovering unknown coefficients in the wave equations by examining measured samples of the reference solution u_m (measured response).

Recently, many applications of wave propagation in science and engineering disciplines used PINNs which we briefly review here. Haghighat et al. [53] explored the application of PINNs for parameter identification in linear elasticity and nonlinear plasticity. Shukla et al. [63], [64] used PINNs to solve inverse wave problems for identifying and characterizing surface cracks, as well as for the identification of microstructural properties of polycrystalline nickel. Moseley et al. [65] and Rasht-Behesht et al. [66] investigated the use of PINNs for solving the acoustic wave equations. Song et al. [67] employed PINNs to solve the frequency-domain anisotropic acoustic wave equation. Smith et al. [68] and Waheed et al. [69] applied PINNs to the Eikonal equation for first arrival-time prediction and travel time tomography, respectively. Zhang et al. [70] used PINNs to estimate the velocity and density fields based on acoustic wave equations.

Among all the PINNs's work, there is a perceived shortage of studies dedicated to full waveform inversion

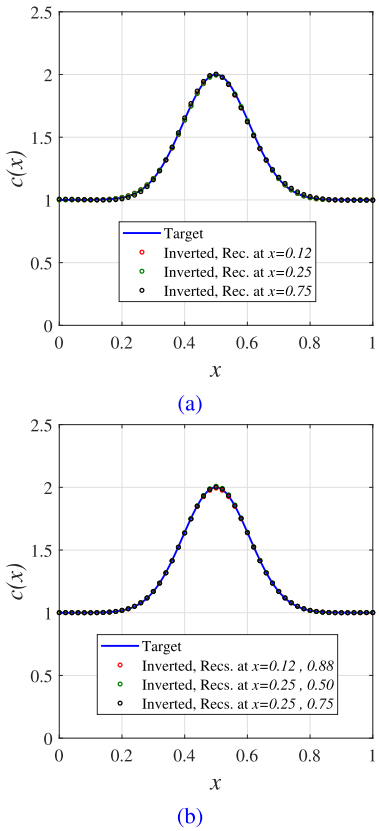

FIGURE 12. Target and inverted wave velocity profiles.

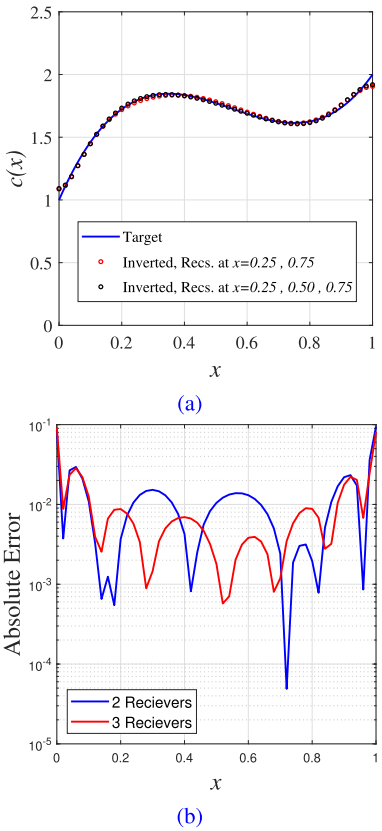

FIGURE 13. (a): Target and inverted wave velocity profiles, (b): Absolute error.

for reconstructing material profiles. The objective of this research is to develop a robust and efficient algorithm based on PINNs' structure for the reconstruction of the wave parameters in heterogeneous finite and unbounded domains.

II. METHODOLOGY

In this section, heterogeneity of media is investigated in three cases. First, the inverse problem is developed for general one-dimensional wave equation. Next, the inversion process in semi-infinite domain is investigated. Finally, we discussed inverted viscously-damped wave motion using PINN scheme.

A. ONE-DIMENSIONAL WAVE PROPAGATION

First, we are interested in to solve the inversion process of the wave propagation in heterogeneous domain (non-constant wave velocity c). We write governing wave Equation along with initial and boundary conditions:

$$\frac{\partial^2 u}{\partial t^2} - \frac{\partial}{\partial x}(c^2 \frac{\partial u}{\partial x}) = 0, \quad x \in [0,1], \quad t \in [0,1]$$
$$u(x,0) = \sin(\pi x), \quad \frac{\partial u}{\partial t}(x,0) = 0$$
$$u(0,t) = 0, \quad u(1,t) = 0$$

Since u is a function of x and t, and c is a function of x, we define two fully connected feed-forward neural networks, one to train for $u(x,t)$ and the other to train for $c(x)$. A set of randomly selected training data points is used as input for both networks, and the output of both networks are employed for automatic differentiation using backpropagation. Visualization of PINNs for solving this problem is presented in Figure 1. For all the cases in this study, we use hyperbolic tangent for activation function and L-BFGS as optimization algorithm. The loss function is considered as:

$$\$ = \frac{1}{N_u}\sum_{i=1}^{N_u} |BI(x^i,t^i)|^2 + \frac{1}{N_\Lambda}\sum_{j=1}^{N_\Lambda} |f(x^j,t^j)|^2 + \frac{1}{N_m}\sum_{i=1}^{N_r}\sum_{k=1}^{N_m} |u_m(i,t^k) - \hat{u}(i,t^k)|^2$$

where

BI = boundary and initial conditions,
f = wave PDE,
u_m = measured displacement response,
$\hat{u}$ = training displacement response,
N_u = number of training points for boundary and initial conditions,
N_Λ = number of training points for PDE (collocation points),
N_r = number of receivers (stations of measured response),
N_m = number of measured responses per receiver.

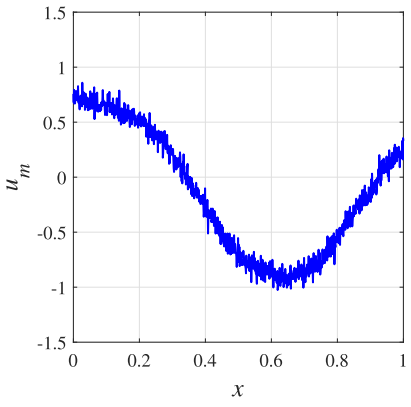

(a) 5% Noise

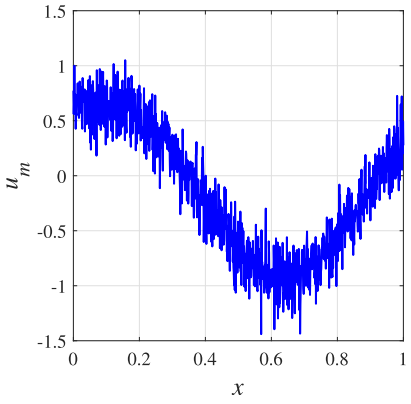

(b) 10% Noise

FIGURE 14. Noisy measured response at $x = 0.25$.

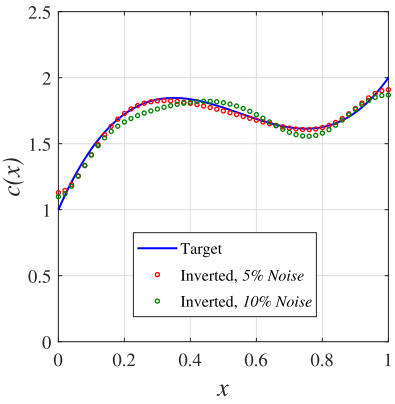

FIGURE 15. Target and inverted wave velocity profiles.

B. WAVE PROPAGATION IN SEMI-INFINITE AND INFINITE MEDIA

Numerical methods, such as Galerkin [25], handle the weak form of PDEs. As a result of the energy nature of the functional in the Galerkin method, the boundary without prescribed displacement or traction will be treated as free surface since it has no contribution to the total potential energy. Constructing the integration terms in weak form requires lower and upper limits, and these limits are obtained by boundary conditions of the domain. Therefore, to solve

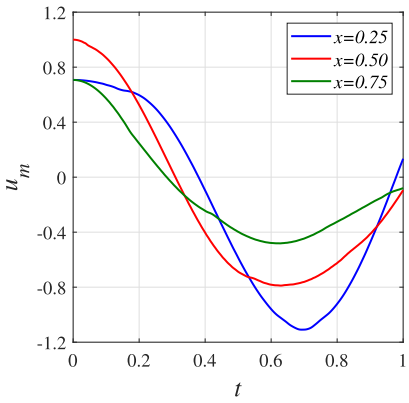

FIGURE 16. Measured displacement responses at three stations.

a wave propagation problem in infinite/semi-infinite media, we need to reduce the domain to a truncated computation domain. To this end, we can employ the enlargement of the computation domain to avoid the wave refection issue. These treatments would result in complicated numerical implementation or unnecessary computational burden for uninterested regions. After the 1950s, some schemes such as transparency conditions [71] and artificial absorbing layers [72] were introduced to resolve the wave reflection issue and avoid utilizing enlarged domains. These approaches result in new strong forms of PDEs including some tuned coefficients and need complicated numerical implementation. As discussed earlier, PINN deals with the strong form of PDEs directly so that we are allowed to apply boundary conditions on only part of the domain boundaries. Any portion of a domain without boundary conditions even for both ends can easily be implemented by PINN. We just do not specify boundary training data points at ends where there is no boundary conditions, and data points at ends are considered as collocation points. This feature would be extremely advantage of PINN in comparison to traditional numerical methods especially for solving the problems with iterative steps such as full waveform inversion that involves infinite or semi-infinite domain.

Figures 2 and 3 schematically represent how the governing equation of wave motion for an interest domain embedded in semi-infinite/infinite media is modeled by PINN and numerical schemes. As seen, when we use the PINN method entire the computational domain plays the role of our interest domain whereas traditional numerical approaches such as FEM needs an enlarged computational domain to satisfy the boundary conditions which increases the computational cost. In our current PINNs algorithm, we just modify the loss function by eliminating the boundary condition(s). To study the sufficiency and accuracy of the PINN for wave equation in semi-infinite domain, Figure 4 provides a comparison between the displacement u computed based on PINN method in a domain of interest against the displacement u computed based on FEM in an enlarged domain. The agreement is excellent.

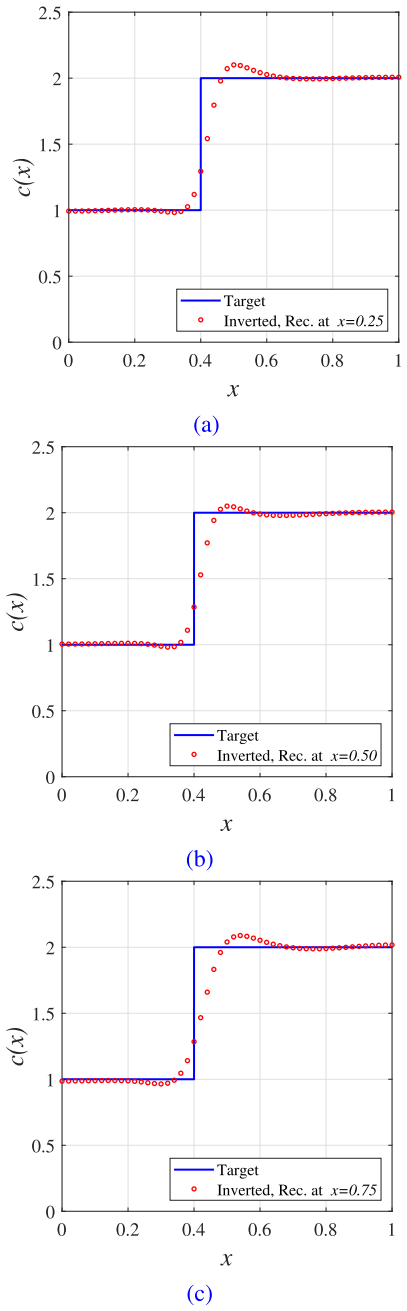

FIGURE 17. Target and inverted wave velocity profiles.

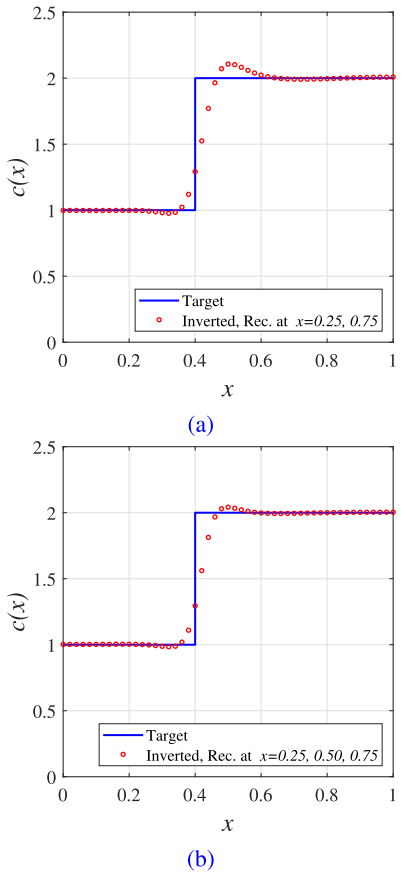

FIGURE 18. Target and inverted wave velocity profiles.

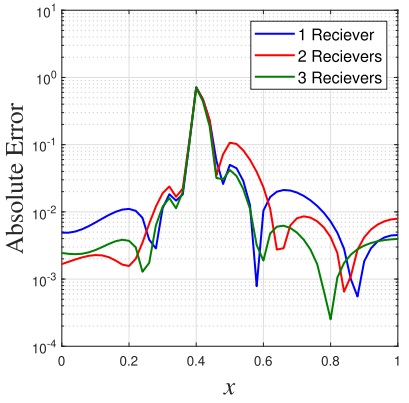

FIGURE 19. Absolute error.

C. VISCOUSLY DAMPED WAVE PROPAGATION

Next, we are interested in to implement the inversion process for viscously damped wave propagation in heterogeneous media (considering unit mass density ($\rho = 1$)):

$$\frac{\partial^2 u}{\partial t^2} - \frac{\partial}{\partial x}(E\frac{\partial u}{\partial x}) + \eta\frac{du}{dt} = 0, \quad x \in [0,1], \quad t \in [0,1]$$
$$u(x,0) = \sin(\pi x), \quad \frac{\partial u}{\partial t}(x,0) = 0$$
$$u(0,t) = 0, \quad u(1,t) = 0$$

Since u is a function of x and t, and E and η are only functions of x, we define two fully connected feed-forward neural networks, one to train for $u(x,t)$ and the other to train E and η, simultaneously. A set of randomly selected training data points is used as input for both networks, and the output of both networks are employed for automatic differentiation using backpropagation. The structure of PINNs for viscously damped motion in heterogeneous domain is provided in Figure 5. The loss function which was introduced earlier for

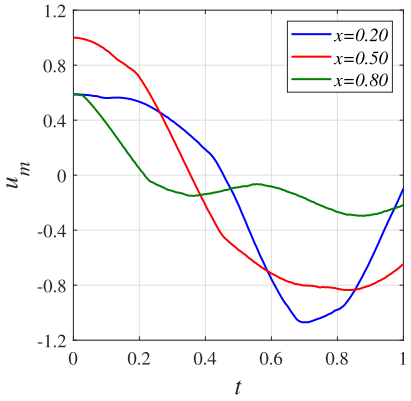

FIGURE 20. Measured displacement responses at three stations.

undamped case is utilized for this case as well with modifying the wave PDE f based on viscously damped motion.

III. NETWORK ARCHITECTURE AND TRAINING DATA SET

In this study, our goal is to investigate the inverse PINNs using only the wave equations. For better comparison and avoiding computational cost, the length of the domain of interest and time of the simulation in all numerical examples is set as one unit. To evaluate the PINNs algorithm, we construct the numerical examples with different types of material profiles (domain's heterogeneity). Of course, changing the network architecture and training data set in each example may obtain better results, but it is a big issue and a negative point that shows we continuously need tuning the problem to improve the results. Therefore, we use a consistent network architecture and training data points for all the numerical examples. For adjusting an appropriate number of hidden layers, neurons, and training data set for inverse PINNs problems, we first implemented some simple forward PINNs examples for our domain of interest with different types of network architecture and training data set. For verification, we compared the results with exact solutions and Finite Element Method. Finally, we adjusted the fixed following parameters for all the examples in this work:

number of hidden layers $= 3$,
number of neuron per layer $= 20$,
$N_u = 800$,
$N_\Lambda = 2000$,
$N_m = 1001$.

IV. NUMERICAL EXAMPLES

In this section, we present several numerical examples of full waveform inversion in heterogeneous media based on the above cases that were discussed.

A. RECONSTRUCTING LINEAR WAVE VELOCITY

We first consider a heterogeneous domain where the wave velocity varies linearly with x, which is assumed as the target wave velocity profile for the inversion process. Figure 6 shows the measured displacement response u_m at $x = 0.5$,

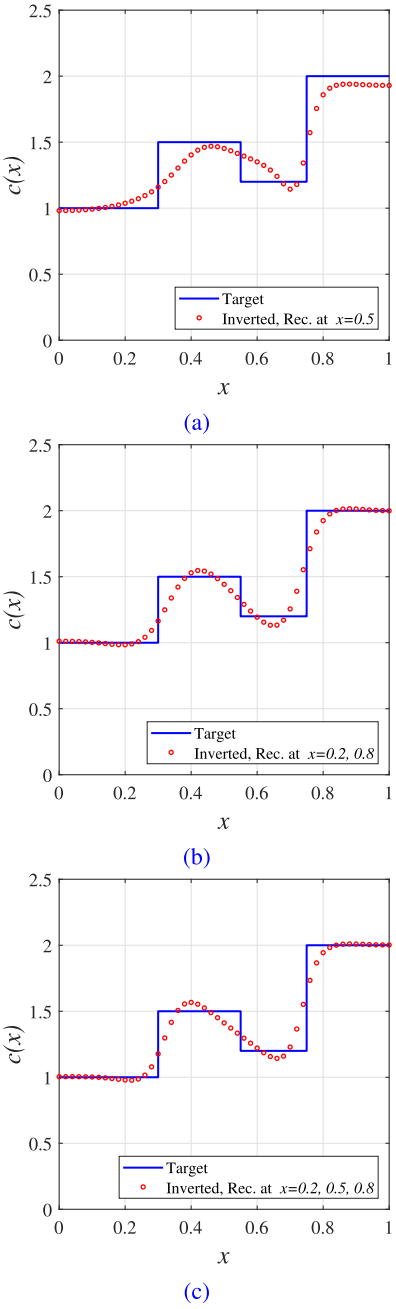

FIGURE 21. Target and inverted wave velocity profiles.

which we obtained by solving the forward problem using Finite Element Method (FEM).

Figure 7 shows the reconstructed wave velocity profiles (red dots) of the domain using the PINNs. In this case, we use one receiver at $x = 0.5$. As seen in the figure, the true profile (blue line) is recovered well using PINN scheme. The value of L^2 norm error is equal to 0.0329.

B. RECONSTRUCTING SMOOTH WAVE VELOCITY

Next, we are interested in to implement the full waveform inversion when parameter c varies smoothly with x. We do this study in several cases.

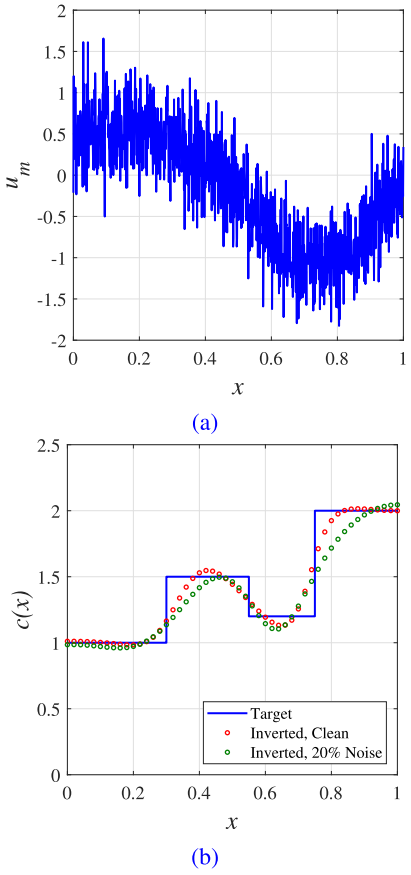

FIGURE 22. (a): Noisy measured response at $x = 0.2$, (b): Target and inverted wave velocity profiles.

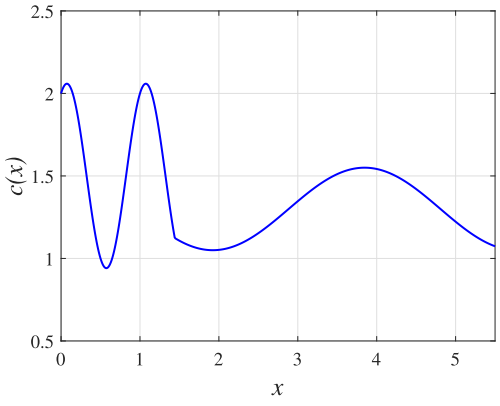

FIGURE 23. Target wave velocity profile $c(x)$.

First, we define the spatial variation of wave velocity as

$$c(x) = 1 + e^{-(\frac{x-0.5}{0.4})^2} \tag{1}$$

For inversion process to recover the target $c(x)$ profiles, we need some samples of measured displacement responses by solving the forward problem (FEM). Figure 8 depicts the measured responses in three sample stations.

We first do the inversion process three times separately. In each attempt, we use the measured response only from one receiver at different location. The reconstruction of c and absolute error are shown in Figure 9. As seen, the wave velocity is properly recovered for all the cases. The maximum errors are observed at both ends, and there is also a small gap between inverted and true profiles at pick point in the middle. These results demonstrate that even one sensor to collect the measured response can successfully recover the target profile.

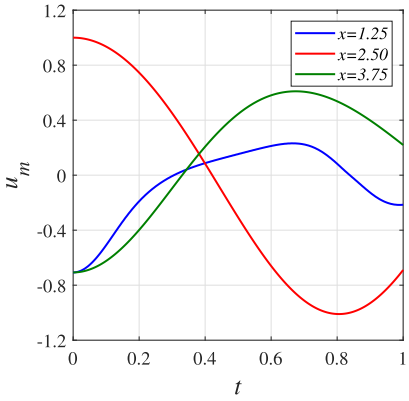

FIGURE 24. Measured displacement responses at three stations.

Next, the number of receivers is increased to two. Figure 10a shows the reconstructed profiles are desirable. Similar to the previous cases, the maximum amount of errors occur at ends and middle of the domain. It is interesting to note that all the recovered profiles are very similar, and locations of the sensors do not do not significantly impact the quality of the results.

Then, the number of receivers is increased to three. The result in this case shows that the profiles are recovered well (Figure 11a) and slightly better when compared to the results obtained using two receivers, presented in Figure 10a. The values of L^2 norm errors for all cases of this example are provided in Table 1. In summary, the target profile is recovered well for all cases and the performance with accuracy of the reconstructed profiles are very close to each other. Increasing the number of sensors slightly reduce the errors, and maximum errors appear on boundaries and middle of the domain.

Now, we modify Equation (1) as below to have a wave velocity target profile as a bell-shaped curve with two flat regions at both ends.

$$c(x) = 1 + e^{-(\frac{x-0.5}{0.15})^2}$$

In this experiment, we investigate the inversion process with several cases of placing one and two receivers in the domain to obtain the measured responses from forward problem. Figure 12 depicts the accurately reconstructed wave velocity, which is practically indistinguishable from the target c. Table 2 summaries L^2 norm errors for all cases.

Finally, we consider a heterogeneous domain with nonlinear third order wave velocity target profile as

$$c(x) = 7.2727x^3 - 12x^2 + 5.7273x + 1$$

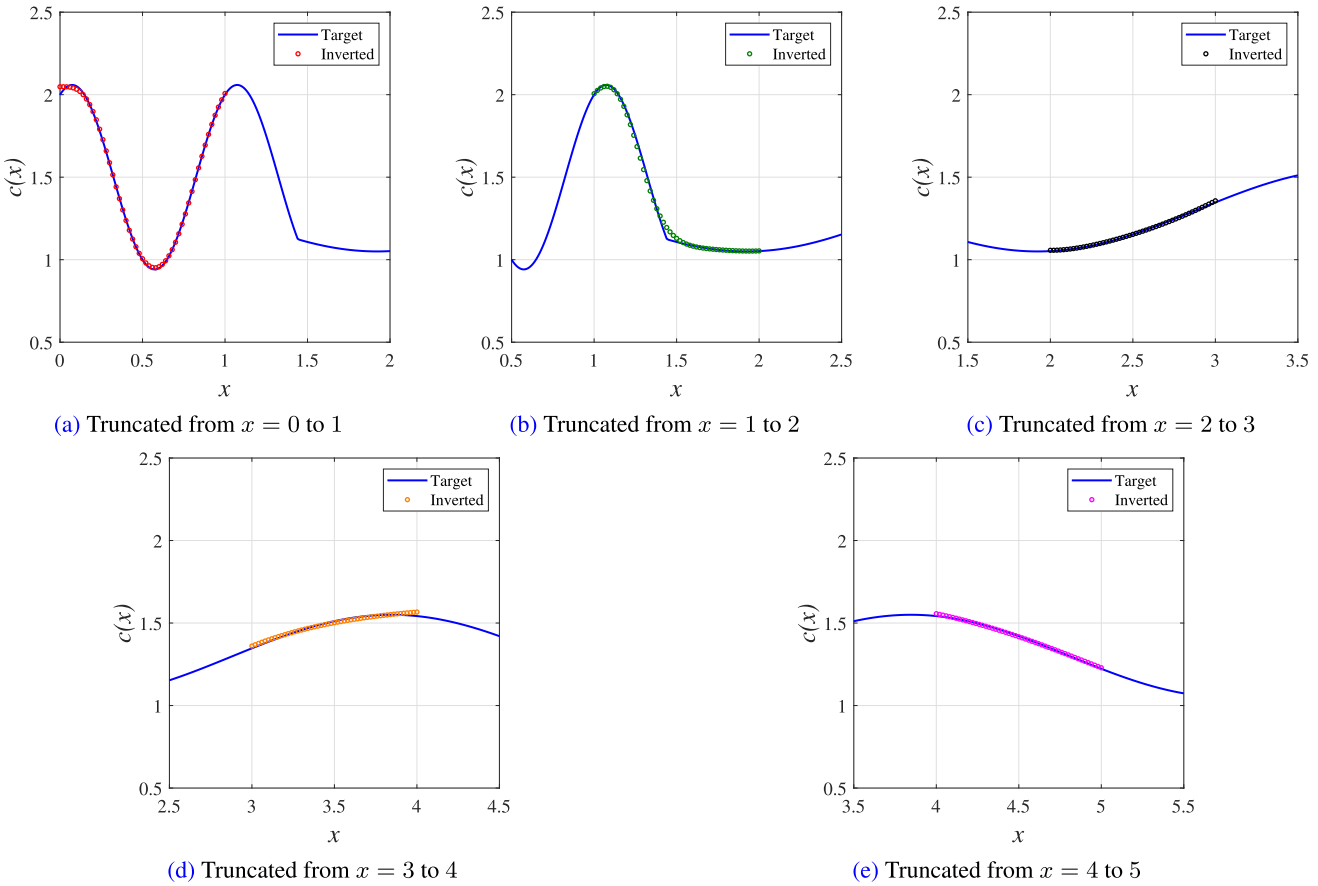

(a) Truncated from $x = 0$ to 1 (b) Truncated from $x = 1$ to 2 (c) Truncated from $x = 2$ to 3

(d) Truncated from $x = 3$ to 4 (e) Truncated from $x = 4$ to 5

FIGURE 25. Target and inverted wave velocity profiles.

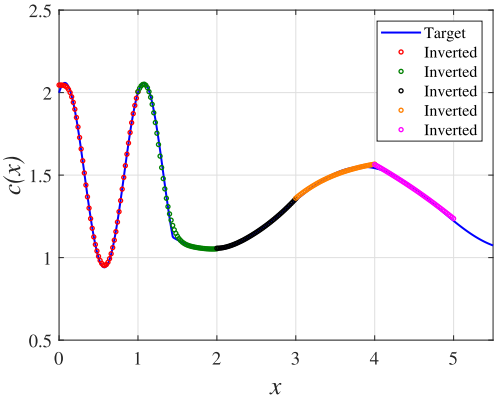

FIGURE 26. Target and inverted wave velocity profiles.

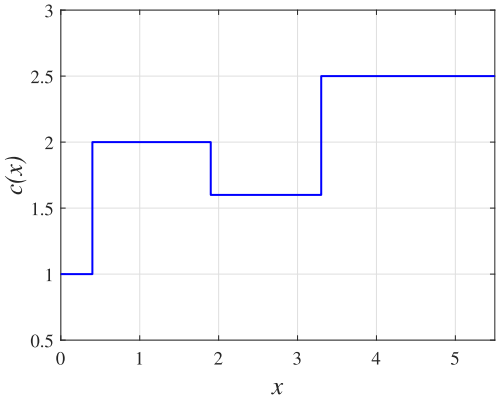

FIGURE 27. Target wave velocity profile $c(x)$

We use two and three receivers to store the measured responses from forward problem. Figure 13a compares the inverted profiles against the target profile. Both cases recovered the true profile fairly well. There are some gaps between the inverted and true results at both ends of the domain, otherwise the inverted results match with target profile. Figure 13b also states absolute error for both cases.

Next, the effect of noise on the PINN full-waveform inversion is investigated. To this end, inversion was performed using the measured responses contaminated by 5% and 10% Gaussian noise as shown in Figure 14. Two receivers are used to collect the measure responses from the forward problem. The inverted profile exhibits smooth variation even in the presence of 10% noise as seen in Figure 15. The wave velocity is fairly reconstructed with 5% noise, however, in the case of

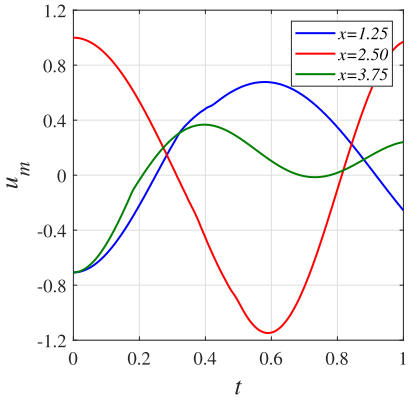

FIGURE 28. Measured displacement responses at three stations.

TABLE 3. L^2 norm error in the recovered c for truncated domains.

Truncated Domain	L^2 norm
$0-1$	0.0713
$1-2$	0.1391
$2-3$	0.0204
$3-4$	0.0694
$4-5$	0.0350

TABLE 4. Predicted damping coefficient for different locations of receivers.

Location (x)	Predicted η	% error
0.25 , 0.75	0.398663	0.334
0.25 , 0.50 , 0.75	0.400912	0.228

10% noise is also acceptable. The values of L^2 norm errors are equal to 0.2209 and 0.3464 for 5% and 10% Gaussian noise, respectively.

C. RECONSTRUCTING LAYERED WAVE VELOCITY

One of the interesting inverse problems in heterogeneous media involves attempting to reconstruct sharp (discontinuous) profiles. In this section, we want to investigate the ability of PINN to invert the layered wave velocity profile. As a first attempt, we are interested in recovering a 2-layer domain with sharp interfaces between the layers. Again, we solve the forward problem (FEM) to obtain the measured displacement response u_m (Figure 16).

Figures 17 and 18 compare the reconstructed wave velocity profiles with target profile. In Figure 17, the inverted profiles are depicted based on measured response from only one sensor at three various stations. Figure 18 presents the behavior of the inversion process as the number of sensors increases. As seen in all cases, the target 2-layer profiles are reasonably well captured, and the algorithm is able to recover the sharp discontinuities in the target profile. The results also suggest that this problem can be stable even when the measured response is collected from only one receiver. Figure 19 presents absolute errors for three cases of measured response by one receiver at $x = 0.50$, two receivers at $x = 0.25, 0.50$, and three receivers at $x = 0.25, 0.50, 0.75$. As expected, maximum errors are observed in the discontinuous region.

TABLE 5. L^2 norm error in the recovered c for different locations of receivers.

Location (x)	L^2 norm E	L^2 norm η
0.25 , 0.75	0.2001	0.2598
0.25 , 0.50 , 0.75	0.1758	0.1902
0.12 , 0.25 , 0.75 , 0.88	0.1621	0.0330

Next, we suppose a 4-layer domain with sharp interfaces between the layers and define the spatial variation of the wave velocity as

$$c(x) = \begin{cases} 1 & \text{for } 0 \le x \le 0.3 \\ 1.5 & \text{for } 0.3 \le x \le 0.55 \\ 1.2 & \text{for } 0.55 \le x \le 0.75 \\ 2 & \text{for } 0.75 \le x \le 1 \end{cases}$$

Figure 20 shows the measured displacement responses at three sample locations on the domain. Figure 21 depicts the reconstructed profiles using one, two, and three sensors to collect the measured responses. As observed, the target profile cannot be captured desirable when one sensor is employed. The inverted profiles which are obtained by two and three receivers are reasonably well, however, the sharp interfaces may not be well reconstructed. The zigzag behavior of the target profile in the middle appears to make the inversion process challenging for reconstructing layers two and three. It is expected that increasing the number of receivers can overcome this issue and lead to a better approximation for the recovered profile, however, in this study, we limited the number of the receivers to maximum three for the elastic profile in a domain of interest with one-unit length.

Finally, the effect of noise on the quality of the inverted profile is investigated. To this end, 20% Gaussian noise is injected to the original measured responses. Figure 22a shows the noise-polluted displacement responses at one sample location in the domain ($x = 0.2$). Figure 22b shows the reconstructed profile using two sensors at $x = 0.2$ and $x = 0.8$. As seen in the figure, the inverted profile obtained from the noisy measurements is not as accurate as the noise-free results but is still quite acceptable.

D. RECONSTRUCTING SMOOTH WAVE VELOCITY IN SEMI-INFINITE MEDIA

Here, we consider a semi-infinite domain with a target wave velocity as shown in Figure 23. We are interested in recovering the target profile from $x = 0$ to $x = 5$. Figure 24 represents the displacement measured responses at some sample points. Similar to the previous examples, we perform the inversion process for each unit interval of the domain. The implementations to obtain the inverted profiles have been conducted separately five times, covering the intervals from

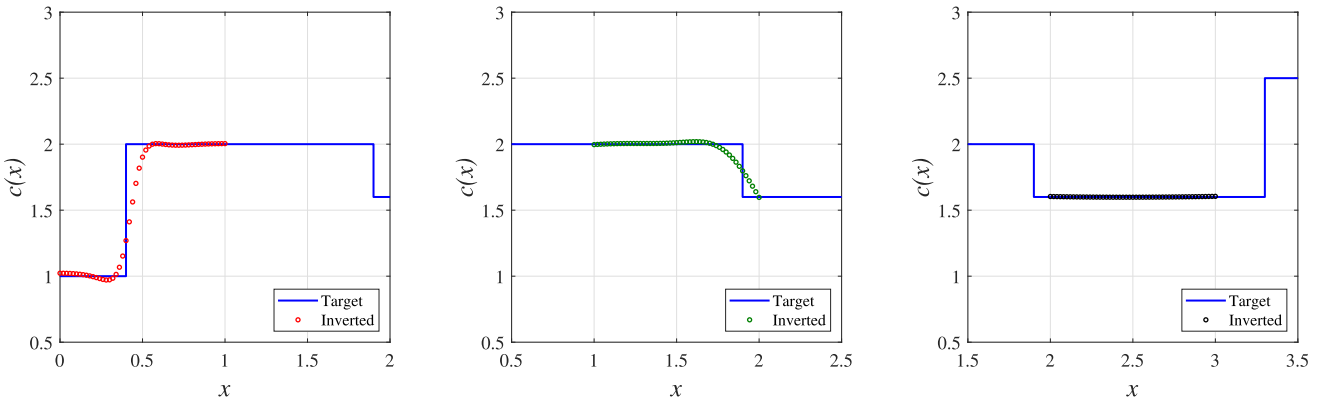

(a) Truncated from $x = 0$ to 1 (b) Truncated from $x = 1$ to 2 (c) Truncated from $x = 2$ to 3

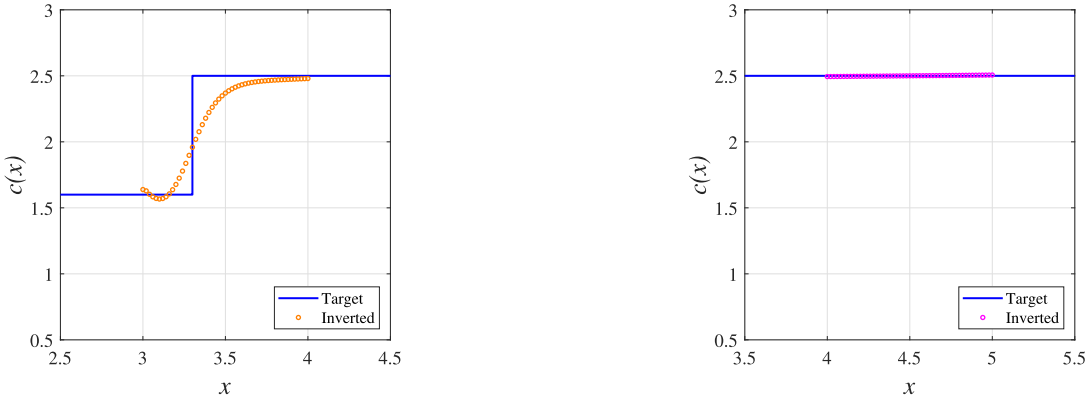

(d) Truncated from $x = 3$ to 4 (e) Truncated from $x = 4$ to 5

FIGURE 29. Target and inverted wave velocity profiles.

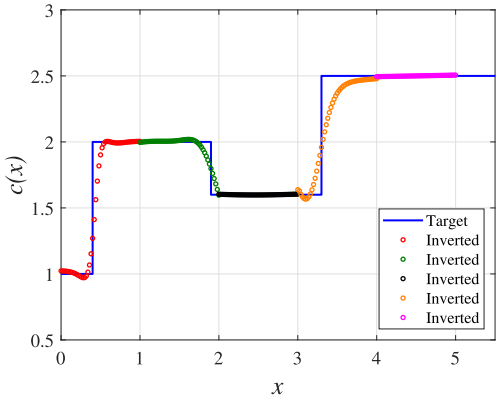

FIGURE 30. Target and inverted wave velocity profiles.

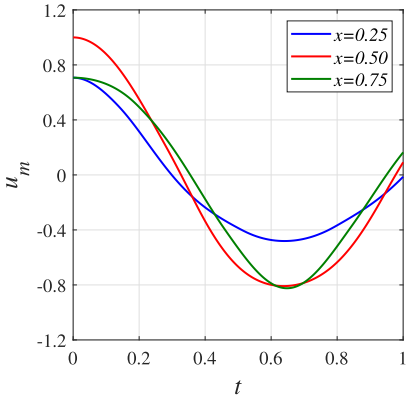

FIGURE 31. Measured displacement responses at three stations.

$x = 0$ to 1, $x = 1$ to 2, $x = 2$ to 3, $x = 3$ to 4, and $x = 4$ to 5. For each case, we consider 3 hidden layers with 20 neurons per each for network architectures, and the total randomly selected number of training and collocation points are $N_u = 800$ and $N_\Lambda = 2000$, respectively. Regarding the geometry of our domain, we only assign the boundary training points at $x = 0$ for the first region ($x = 0$ to 1). Three receivers with $N_m = 1001$ per each are used for measured responses in each truncated domain.

Accordingly, we reconstruct $c(x)$ profiles shown in Figure 25 corresponding to five truncated domains of interest. In each region, the reconstructed profile adequately captures the target wave velocity of the interest domain. Table 3 also summaries L^2 norm errors for all cases.

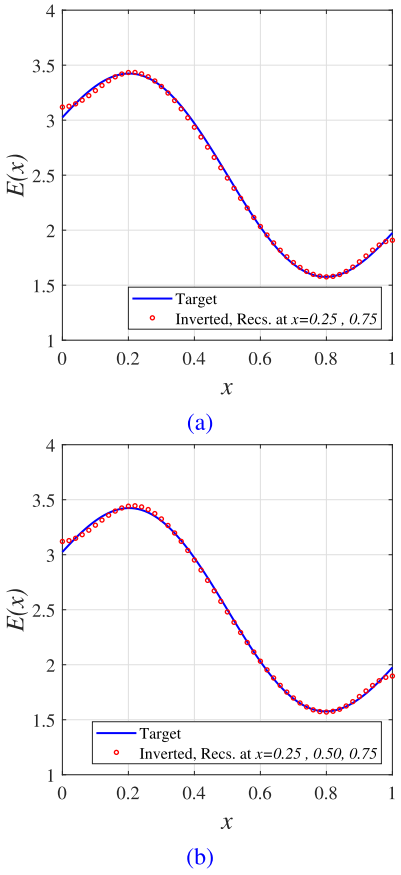

FIGURE 32. Target and inverted elastic modulus profiles.

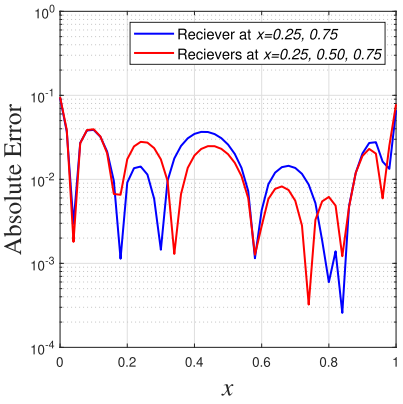

FIGURE 33. Absolute error.

Figure 26 combines all the inverted profiles of the truncated domains.

E. RECONSTRUCTING LAYERED WAVE VELOCITY IN SEMI-INFINITE MEDIA

Here, we want to recover a 4-layer interest domain ($x = 0$ to 5) which is embedded in a semi-infinite media as shown in Figure 27. The displacement measured responses at three sample stations are provided in Figure 28, and the receiver at each station collects $N_m = 1001$ displacement response.

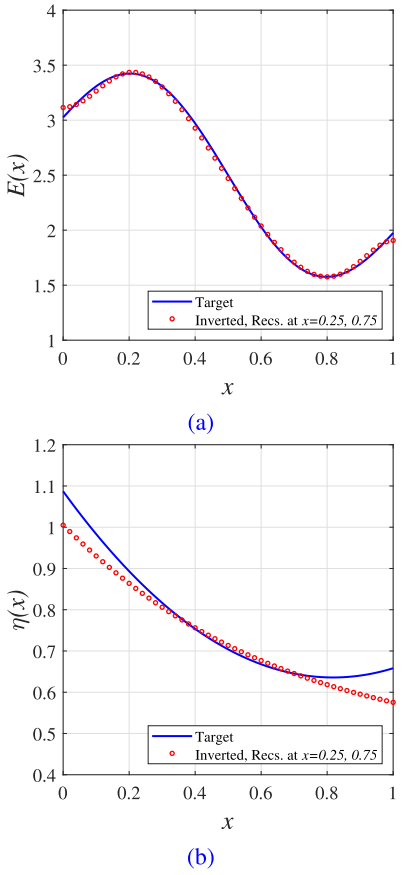

FIGURE 34. (a): Target and inverted $E(x)$, (b): Target and inverted $\eta(x)$.

We divide the domain of interest into five truncated domains with equal unit lengths. Similar to the previous example, the inversion procedure is applied separately to each truncated domain. Three hidden layers with 20 neurons per each layer is assumed as network architectures including $N_u = 800$ and $N_\Lambda = 2000$ for training and collocation points, respectively.

The inverted profiles of the one unit truncated domains are separately provided in Figure 29. The true profile is reconstructed fairly well in the continuous regions. As noted before, one of the interests here is the ability to recover the sharp discontinuities in the target profile. As shown in the figures, the PINN scheme captures the sharply varying profile reasonably well. Lastly, the combination of the recovered profiles of the truncated domains is depicted in Figure 30.

F. RECONSTRUCTING SMOOTH E AND CONSTANT η

First, we are interested in implementing the full damped waveform inversion when target elastic modulus E varies smoothly as defined in Equation (2), while the target damping coefficient is assumed to be constant $\eta = 0.4$.

$$E(x) = 2.5 + 0.525\sin(2\pi x) + 0.525\cos(\pi x) \qquad (2)$$

Figure 31 depict the measured responses in three sample stations by solving the forward problem (FEM). Since u is a function of x and t, and E is a function of x, we define two

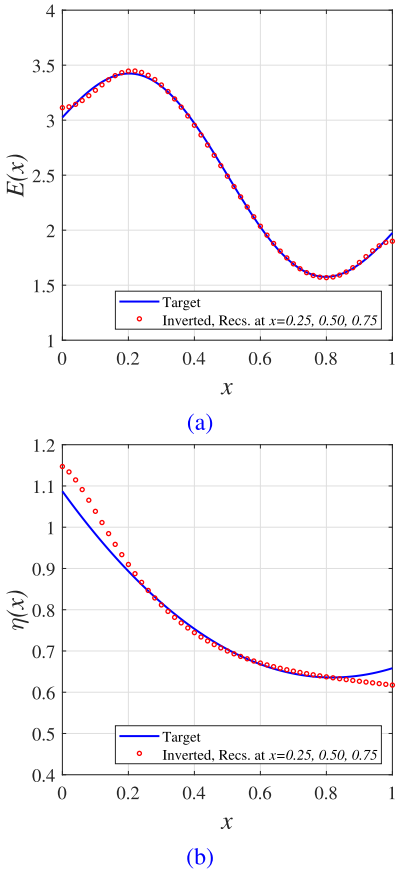

FIGURE 35. (a): Target and inverted $E(x)$, (b): Target and inverted $\eta(x)$.

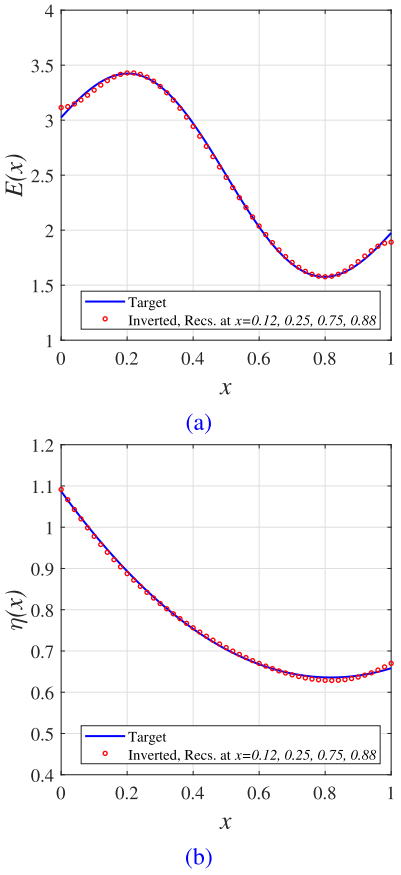

FIGURE 36. (a): Target and inverted $E(x)$, (b): Target and inverted$\eta(x)$.

fully connected feed-forward neural networks, one to train for $u(x,t)$ and the other to train for $E(x)$. Figure 32 shows the reconstructed elastic modulus profiles using two and three sensors in the domain. Both cases capture the smooth target E profile very well. Figure 33 illustrates the absolute error for both cases, and as shown, the maximum errors occurs at the boundaries. The results of inverted damping coefficients are provided in Table (4) which are very close to the target value. The values of L^2 norm errors are equal to 0.1829 and 0.1779 in the cases of two and three receivers, respectively.

G. RECONSTRUCTING SMOOTH E AND η

Now, we are interested in simultaneously reconstructing both smooth E and η target profiles. E and η profiles smoothly vary as defined in Equation (2) and (3), respectively.

$$\eta(x) = 0.6749x^2 - 1.1038x + 1.0871 \tag{3}$$

We first use two sensors at $x = 0.25$ and $x = 0.75$ for time-history measured responses. Figure 34 depicts reconstructed profiles for $E(x)$ and $\eta(x)$. As seen, while the function $E(x)$ is well reconstructed, there is room for improvement in the inverted function $\eta(x)$. To this end, we increase the number of receivers to three and four and implement the inversion procedure. The accuracy of $\eta(x)$ using three receivers for measured responses is slightly better than before (Figure 35). Four receivers capture both smooth target profiles $E(x)$ and $\eta(x)$ very well (Figure 36). The values of L^2 norm errors for both E and η are provided in Table 5.

H. RECONSTRUCTING LAYERED E AND η

Next, we attempt to recover sharp heterogeneous target profiles of elastic modulus and damping coefficient. Figure 37 depicts a 2-layer domain with sharp interfaces between the layers. Again, we solve the forward problem (FEM) to obtain the measured displacement response u_m (Figure 38), which is used for inversion process.

However, the goal of this example is the reconstruction of both target profiles. We first assume that we are more interested in recovering only the elastic modulus profile and an approximate value of the damping coefficient. In other words, using the current measured responses obtained from two heterogeneous parameters, we aim to investigate the ability of PINN to recover one heterogeneous profile and one approximated scalar value. Figure 39 shows the inverted elastic modulus profile of the layered medium using two sensors at $x = 0.25$ and $x = 0.75$ to collect the measured responses of the forward problem. As seen, the result is fairly

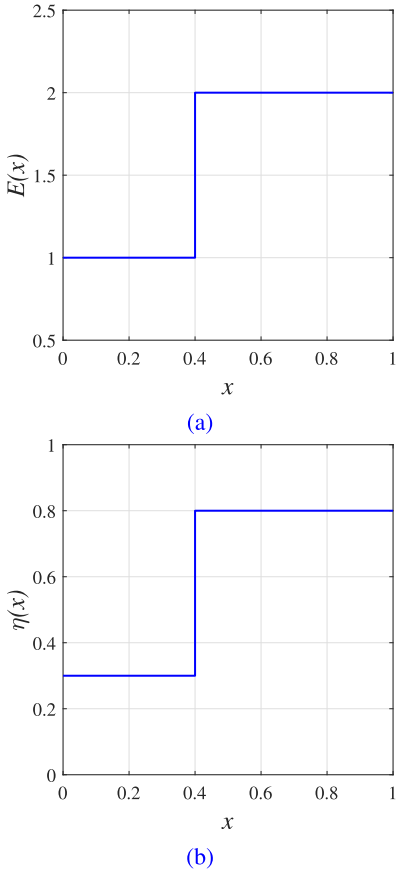

FIGURE 37. (a): Target profile of $E(x)$, (b): Target profile of $\eta(x)$.

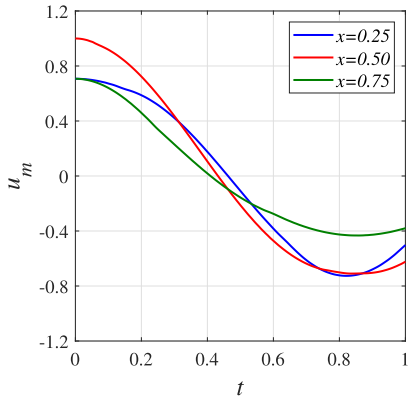

FIGURE 38. Measured displacement responses at three stations.

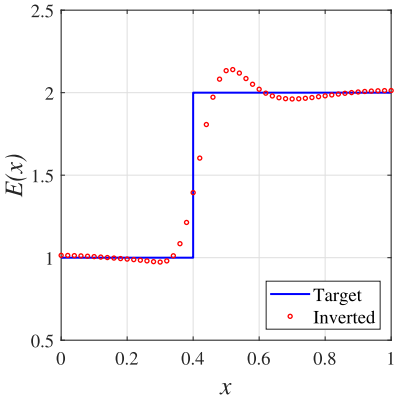

FIGURE 39. Target and inverted elastic modulus profiles.

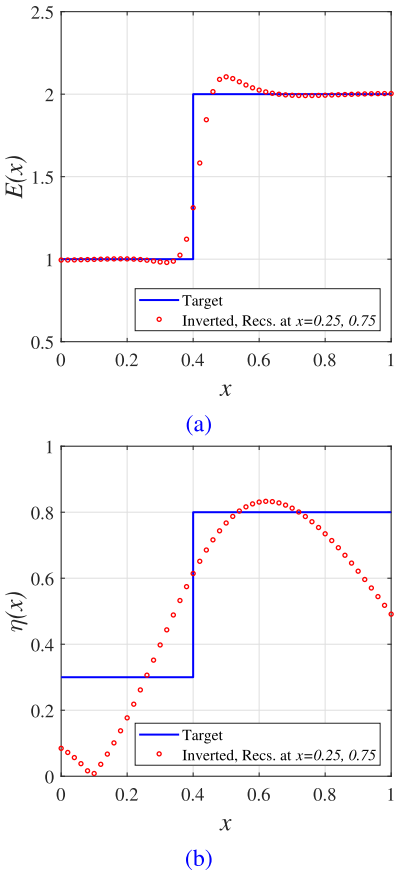

FIGURE 40. (a): Target and inverted $E(x)$, (b): Target and inverted $\eta(x)$.

good even when considering a non-heterogeneous domain for the damping coefficient. The output value for η is equal to 0.563 which is within the range of exact target profile of η.

Finally, it is sought to reconstruct both heterogeneous profiles E and η. For the inversion process, we employ the measured responses from two receivers at $x = 0.25$ and $x = 0.75$. Figure 40 shows inverted profiles for $E(x)$ and $\eta(x)$. As shown in the figure, $E(x)$ is well reconstructed, while $\eta(x)$ is poorly recovered. Then, we use the measured responses from three stations and repeat the inversion process. The results (Figure 41) indicate that, although the performance of the inverted $\eta(x)$ is better than in the previous case, it is still not entirely accurate. Next, the problem will be redone using the measured responses from four receivers. Both reconstructed profiles are depicted in Figure 42 which states the recovered $\eta(x)$ is fairly desirable in this case. In summary, attempting to perform the inversion process simultaneously for multiple parameters in a heterogeneous domain may require an increase in the number of receivers to collect the measured responses.

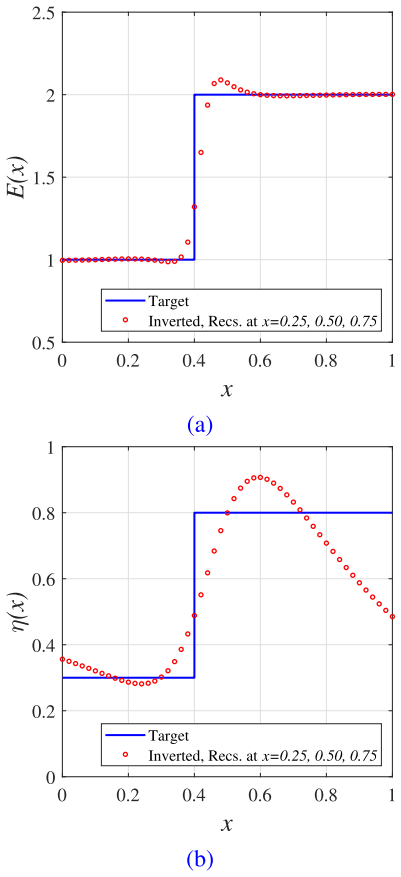

FIGURE 41. (a): Target and inverted $E(x)$, (b): Target and inverted $\eta(x)$.

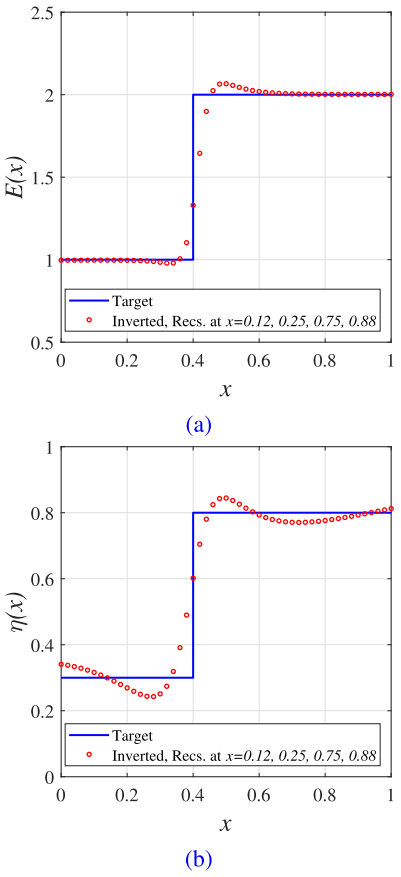

FIGURE 42. (a): Target and inverted $E(x)$, (b): Target and inverted $\eta(x)$.

V. CONCLUSION

In this study, we investigated inverse problems for wave equations in heterogeneous media using physics informed neural networks. For all the inverse problems, we obtain the time-history displacement measured response by solving the forward problem with FEM. We developed an algorithm based on PINN for solving the inverse wave equation in heterogeneous domain. In the first case, the aim was to reconstruct the wave velocity target profile $c(x)$ for the entire domain. We assessed inversion process for both continuous and piecewise continues target profiles. Displacement measured responses from forward problem were used at some certain locations in the domain. Numerical results implied that the algorithm worked well in efficiently capturing the target profiles. One receiver to collect measured response seems to be enough to obtain the suitable recovered profile, however, increasing the numbers of the receivers improve the accuracy. Two or three receivers could be reasonable for all the cases even with noisy measured responses.

Next, we used PINN to solve the inverse wave equation for a domain of interest embedded in a heterogeneous infinite/semi-infinite media. To model these types of domains, we just need to define collocation points instead of training data points at the end(s) where we do not have fixed boundary condition(s). This is one of the major advantages of PINN in comparison to traditional numerical schemes. To assess the performance of the algorithm for this problem, we assumed a semi-infinite domain and applied the inversion procedure with both continuous and piecewise continuous target wave velocity profiles. For both cases, we attempted to reconstruct the target wave velocity for five separate truncated domains with a unit length from $x = 0$ to $x = 5$. The measured responses were obtained by solving the forward problem in an enlarged domain with FEM, and the results indicated that PINN was able to recover the target profiles fairly well.

The last objective was a full waveform inversion approach for reconstructing elastic modulus and viscous damping coefficient subject to PDEs that govern the motion of viscously damped wave propagation. Regarding the heterogeneous domain, we investigated two cases. First, the inversion process was performed for smooth $E(x)$ profile and constant η. This means that we supposed the domain's heterogeneity depended solely on E. However, the algorithm simultaneously reconstructed $E(x)$ and predicted η. Utilizing measured response from two receivers could properly capture both target E profile and coefficient η value. Then, we considered heterogeneity for both E and η. To this end, we supposed two cases smooth and layered target profiles for E and η. Difficulties in simultaneous inversion arose in the example

provided. Specifically, the reconstructed E profile was easily obtained using only two receivers, but these two receivers could not produce an acceptable recovered profile for η. Increasing the number of sensors to four could successfully overcome this issue and provide the desirable output for the profile of η as well.

REFERENCES

[1] R. C. Qiu, Z. Hu, H. Li, and M. C. Wicks, "Convex optimization," in *Cognitive Radio Communication and Networking: Principles and Practice*. Cambridge, U.K.: Cambridge Univ. Press, 2013, pp. 235–282.

[2] A. Cauchy, "Methode generale pour la resolution des systemes de' equations simultanées," *Comp. Rendus de l'Academie des Sci.*, vol. 25, pp. 536–538, Jul. 1847.

[3] W. Rudin, *Principles of Mathematical Analysis*. New York, NY, USA: McGraw-Hill, 1976.

[4] P. F. Verhuls, "Notice sur la loi que la population suit dans son accroissement," *Correspondance mathematique Et Phys.*, vol. 10, pp. 113–121, 1838.

[5] D. P. Kingma and J. L. Ba, "Adam: A method for stochastic optimization," in *Proc. 3rd Int. Conf. Learn. Represent.*, pp. 1–14 2015.

[6] J. Kiefer and J. Wolfowitz, "Stochastic estimation of the maximum of a regression function," *Ann. Math. Statist.*, vol. 23, no. 3, pp. 462–466, Sep. 1952.

[7] H. Robins and S. Monro, "A stochastic approximation method," *Ann. Math. Statist.*, vol. 22, no. 3, pp. 400–407, 1951.

[8] A. N. Tikhonov and V. Y. Arsenin, *Solutions of Ill-posed Problems*. Hoboken, NJ, USA: Wiley, 1977.

[9] O. M. Alifanov, E. A. Artyukhin, and S. V. Rumyantsev, *Extremal Methods for Solving Ill-Posed Problems*. Moscow, Russia: Nauka, 1988.

[10] A. M. Denisov, "Uniqueness of the solution of the problem of determining the nonlinear coefficient of a system of partial differential equations locally and globally," *Sib. Mat. Zh.*, vol. 36, pp. 60–71, Aug. 1995.

[11] C. W. Groetsch, *Inverse Problems in Mathematical Sciences*. Wiesbaden, Germany: Vieweg, 1993.

[12] J. Hadamard, "Sur les problèmes aux dérivées partielles et leur signification physique," *Princeton Univ. Bull.*, vol. 13, pp. 49–52, Jul. 1902.

[13] M. M. Lavrentiev, "Integral equations of the first kind," *Dokl. Akad. Nauk*, vol. 127, pp. 31–33, Sep. 1959.

[14] J. Radon, "Uber die bestimmung von funktionen durch ihre integralwerte langs gewisser mannigfaltigkeiten. Berichte uber die verhandlungen gesellshaft der wissenschaften zu leipzig," *J. Math. Phys.*, vol. 69, pp. 262–277, Dec. 1917.

[15] M. Hanke and P. C. Hansen, "Regularization methods for large-scale problems," *Surv. Math. for Ind.*, vol. 3, no. 4, pp. 253–315, 1993.

[16] P. C. Hansen, "Analysis of discrete Ill-posed problems by means of the L-curve," *SIAM Rev.*, vol. 34, no. 4, pp. 561–580, Dec. 1992.

[17] W. Menke, *Geophysical Data Analysis: Discrete Inverse Theory*. New York, NY, USA: Academic, 1984.

[18] D. W. Oldenburg, "An introduction to linear inverse theory," *IEEE Trans. Geosci. Remote Sens.*, vols. GE-22, no. 6, pp. 665–674, Nov. 1984.

[19] R. Parker, "Understanding inverse theory," *Annu. Rev. Earth Planet. Sci.*, vol. 5, pp. 35–64, Aug. 1977.

[20] A. N. Tikhonov, "On the stability of inverse problems," *Doklady Acad. Sci. USSR*, vol. 39, pp. 176–179, Dec. 1943.

[21] A. N. Tikhonov, "Solution of incorrectly formulated problems and the regularization method," *Sov. Math. Doklady*, vol. 4, pp. 1035–1038, 1963.

[22] S. Twomey, *Introduction To the Mathematics of Inversion in Remote Sensing and Indirect Measurements*. Amsterdam, The Netherlands: Elsevier, 1977.

[23] R. H. Byrd, P. Lu, J. Nocedal, and C. Zhu, "A limited memory algorithm for bound constrained optimization," *SIAM J. Sci. Comput.*, vol. 16, no. 5, pp. 1190–1208, Sep. 1995.

[24] R. Fletcher, *Practical Methods of Optimization*. Hoboken, NJ, USA: Wiley, 1987.

[25] A. Ern and J. Guermond, *Theory and Practice of Finite Elements*. Cham, Switzerland: Springer, 2004.

[26] G. D. Smith, *Numerical Solution of Partial Differential Equations: Finite Difference Methods*. New York, NY, USA: Oxford, 1978.

[27] T. Bohlen, "Parallel 3-D viscoelastic finite difference seismic modelling," *Comput. Geosci.*, vol. 28, no. 8, pp. 887–899, Oct. 2002.

[28] K. Leng, T. Nissen-Meyer, M. van Driel, K. Hosseini, and D. Al-Attar, "AxiSEM3D: Broad-band seismic wavefields in 3-D global earth models with undulating discontinuities," *Geophys. J. Int.*, vol. 217, no. 3, pp. 2125–2146, Jun. 2019.

[29] B. Farley and W. Clark, "Simulation of self-organizing systems by digital computer," *Trans. IRE Prof. Group Inf. Theory*, vol. 4, no. 4, pp. 76–84, Sep. 1954.

[30] D. O. Hebb, *The Organization of Behavior*. Hoboken, NJ, USA: Wiley, 1949.

[31] W. Mcculloch and W. Pitts, "A logical calculus of the ideas immanent in nervous activity," *Bull. Math. Biol.*, vol. 52, nos. 1–2, pp. 99–115, 1990.

[32] N. Rochester, J. Holland, L. Haibt, and W. Duda, "Tests on a cell assembly theory of the action of the brain, using a large digital computer," *IEEE Trans. Inf. Theory*, vol. IT-2, no. 3, pp. 80–93, Sep. 1956.

[33] F. Rosenblatt, "The perceptron: A probabilistic model for information storage and organization in the brain," *Psychol. Rev.*, vol. 65, no. 6, pp. 386–408, 1958.

[34] K. Hornik, M. Stinchcombe, and H. White, "Multilayer feedforward networks are universal approximators," *Neural Netw.*, vol. 2, no. 5, pp. 359–366, Jan. 1989.

[35] A. G. Ivakhnenko and V. G. Lapa, *Cybernetic Predicting Devices*. New York, NY, USA: CCM Information Corporation, 1965.

[36] K. Hornik, M. Stinchcombe, and H. White, "Universal approximation of an unknown mapping and its derivatives using multilayer feedforward networks," *Neural Netw.*, vol. 3, no. 5, pp. 551–560, Jan. 1990.

[37] A. G. Ivakhnenko and V. G. Lapa, *Cybernetics and Forecasting Techniques*. New York, NY, USA: American Elsevier, 1967.

[38] A. G. Ivakhnenko, "The group method of data of handling; a rival of the method of stochastic approximation," *Sov. Autom. Control*, vol. 13, no. 3, pp. 43–55, 1968.

[39] A. G. Ivakhnenko, "Polynomial theory of complex systems," *IEEE Trans. Syst. Man, Cybern.*, vols. SMC-1, no. 4, pp. 364–378, Oct. 1971.

[40] R. D. Joseph, *Contributions To Perceptron Theory*. Ithaca, NY, USA: Cornell Univ. Press, 1961.

[41] D. E. Rumelhart, G. E. Hinton, and R. J. Williams, "Learning representations by back-propagating errors," *Nature*, vol. 323, no. 6088, pp. 533–536, Oct. 1986.

[42] P. Werbos, *Beyond Regression : New Tools for Prediction and Analysis in the Behavioral Sciences*. Cambridge, MA, USA: Harvard Univ. Press, 1974.

[43] M. Minsky and S. Papert, *Perceptrons: An Introduction to Computational Geometry*. Cambridge, MA, USA: MIT Press, 1969.

[44] B. Widrow and M. Hoff, "Associative storage and retrieval of digital information in networks of adaptive neurons," *Biol. Prototypes Synth. Syst.*, vol. 1, p. 160, Jul. 1962.

[45] I. E. Lagaris, A. Likas, and D. I. Fotiadis, "Artificial neural networks for solving ordinary and partial differential equations," *IEEE Trans. Neural Netw.*, vol. 9, no. 5, pp. 987–1000, Jan. 1998.

[46] M. Raissi, P. Perdikaris, and G. E. Karniadakis, "Physics-informed neural networks: A deep learning framework for solving forward and inverse problems involving nonlinear partial differential equations," *J. Comput. Phys.*, vol. 378, pp. 686–707, Feb. 2019.

[47] A. G. Baydin, B. A. Pearlmutter, A. A. Radul, and J. M. Siskind, "Automatic differentiation in machine learning: A survey," *J. Mach. Learn. Res.*, vol. 18, no. 1, pp. 1–43, 2018.

[48] S. Cai, Z. Wang, S. Wang, P. Perdikaris, and G. E. Karniadakis, "Physics-Informed neural networks for heat transfer problems," *J. Heat Transf.*, vol. 143, no. 6, Jun. 2021, Art. no. 060801.

[49] X. Jin, S. Cai, H. Li, and G. Karniadakis, "Physics-informed neural networks for the incompressible Navier-Stokes equations," *J. Comput. Phys.*, vol. 426, Jul. 2021, Art. no. 109951.

[50] R. Rodriguez-Torrado, P. Ruiz, L. Cueto-Felgueroso, M. C. Green, T. Friesen, S. Matringe, and J. Togelius, "Physics-informed attention-based neural network for hyperbolic partial differential equations: Application to the buckley–leverett problem," *Sci. Rep.*, vol. 12, no. 1, p. 757, May 2022.

[51] Z. Mao, A. D. Jagtap, and G. E. Karniadakis, "Physics-informed neural networks for high-speed flows," *Comput. Methods Appl. Mech. Eng.*, vol. 360, Mar. 2020, Art. no. 112789.

[52] A. D. Jagtap, Z. Mao, N. Adams, and G. E. Karniadakis, "Physics-informed neural networks for inverse problems in supersonic flows," *J. Comput. Phys.*, vol. 466, Oct. 2022, Art. no. 111402.

[53] E. Haghighat, M. Raissi, A. Moure, H. Gomez, and R. Juanes, "A physics-informed deep learning framework for inversion and surrogate modeling in solid mechanics," *Comput. Methods Appl. Mech. Eng.*, vol. 379, Jun. 2021, Art. no. 113741.
[54] Y. Xu, J. Li, and X. Chen, "Physics informed neural networks for velocity inversion," in *Proc. SEG Tech. Program Expanded Abstr.*, Aug. 2019, pp. 2584–2588.
[55] A. D. Jagtap, K. Kawaguchi, and G. E. Karniadakis, "Adaptive activation functions accelerate convergence in deep and physics-informed neural networks," *J. Comput. Phys.*, vol. 404, Mar. 2020, Art. no. 109136.
[56] L. Yang, X. Meng, and G. E. Karniadakis, "B-PINNs: Bayesian physics-informed neural networks for forward and inverse PDE problems with noisy data," *J. Comput. Phys.*, vol. 425, Jan. 2021, Art. no. 109913.
[57] Y. Yang and P. Perdikaris, "Adversarial uncertainty quantification in physics-informed neural networks," *J. Comput. Phys.*, vol. 394, pp. 136–152, Oct. 2019.
[58] F. Sahli Costabal, Y. Yang, P. Perdikaris, D. E. Hurtado, and E. Kuhl, "Physics-Informed neural networks for cardiac activation mapping," *Frontiers Phys.*, vol. 8, pp. 1–17, Feb. 2020.
[59] Y. Chen, L. Lu, G. E. Karniadakis, and L. Dal Negro, "Physics-informed neural networks for inverse problems in nano-optics and metamaterials," *Opt. Exp.*, vol. 28, no. 8, p. 11618, 2020.
[60] J. Yu, L. Lu, X. Meng, and G. E. Karniadakis, "Gradient-enhanced physics-informed neural networks for forward and inverse PDE problems," *Comput. Methods Appl. Mech. Eng.*, vol. 393, Apr. 2022, Art. no. 114823.
[61] L. Lu, X. Meng, Z. Mao, and G. E. Karniadakis, "DeepXDE: A deep learning library for solving differential equations," *SIAM Rev.*, vol. 63, no. 1, pp. 208–228, Jan. 2021.
[62] Y. Qian, Y. Zhang, Y. Huang, and S. Dong, "Physics-informed neural networks for approximating dynamic (hyperbolic) PDEs of second order in time: Error analysis and algorithms," *J. Comput. Phys.*, vol. 495, Aug. 2023, Art. no. 112527.
[63] K. Shukla, P. C. Di Leoni, J. Blackshire, D. Sparkman, and G. E. Karniadakis, "Physics-Informed neural network for ultrasound nondestructive quantification of surface breaking cracks," *J. Nondestruct. Eval.*, vol. 39, no. 3, pp. 1–20, Sep. 2020.
[64] K. Shukla, A. D. Jagtap, and G. E. Karniadakis, "Parallel physics-informed neural networks via domain decomposition," *J. Comput. Phys.*, vol. 447, Dec. 2021, Art. no. 110683.
[65] B. Moseley, A. Markham, and T. Nissen-Meyer, "Solving the wave equation with physics-informed deep learning," 2020, *arXiv:2006.11894*.
[66] M. Rasht-Behesht, C. Huber, K. Shukla, and G. E. Karniadakis, "Physics-informed neural networks (PINNs) for wave propagation and full waveform inversions," *J. Geophys. Res. Solid Earth*, vol. 127, no. 5, pp. 1–19, May 2022.
[67] C. Song, T. Alkhalifah, and U. B. Waheed, "Solving the frequency-domain acoustic VTI wave equation using physics-informed neural networks," *Geophys. J. Int.*, vol. 225, no. 1, pp. 846–859, Dec. 2020.
[68] J. D. Smith, K. Azizzadenesheli, and Z. E. Ross, "EikoNet: Solving the Eikonal equation with deep neural networks," 2020, *arXiv:2004.00361*.
[69] M. Kühbach, P. Bajaj, M. H. Celik, E. A. Jägle, and B. Gault, "On strong scaling and open source tools for analyzing atom probe tomography data," 2020, *arXiv:2004.05188*.
[70] Y. Zhang, X. Zhu, and J. Gao, "Seismic inversion based on acoustic wave equations using physics-informed neural network," *IEEE Trans. Geosci. Remote Sens.*, vol. 61, Jan. 2023, Art. no. 4500511, doi: 10.1109/TGRS.2023.3236973.
[71] R. D. Mindlin and H. H. Bleich, "Response of an elastic cylindrical shell to a transverse, step shock wave," *J. Appl. Mech.*, vol. 20, no. 2, pp. 189–195, Jun. 1953.
[72] J.-P. Berenger, "A perfectly matched layer for the absorption of electromagnetic waves," *J. Comput. Phys.*, vol. 114, no. 2, pp. 185–200, Oct. 1994.

ALIREZA PAKRAVAN received the master's degree in civil engineering from the Amirkabir University of Technology, Tehran, Iran, in 2006, and the Ph.D. degree in structural engineering from New Mexico State University, Las Cruces, NM, USA, in 2014.

From 2015 to 2017, he was a Postdoctoral Researcher with the Department of Structural Engineering, University of California at San Diego, San Diego, CA, USA. He is currently an Adjunct Professor with the Department of Mechanical Engineering, San Diego State University, San Diego. His publications span several research areas and his research interests include related to several topics, including numerical methods in applied mathematics, structural dynamics and wave propagation, inverse problems and optimizations, machine learning, neural networks, and data analysis. He has served as a reviewer for some journal articles.